Electronic Supplementary Material (ESI) for New Journal of Chemistry.
This journal is © The Royal Society of Chemistry and the Centre National de la Recherche Scientifique 2023

Electronic Supplementary Information (ESI) for New Journal of Chemistry

Supplementary Information

A nonfullerene acceptor with π-conjugation extended end groups to access enhanced photovoltaic performance

Chunyan Liu,[a] Zhihui Wu,[a] Nailiang Qiu,*[b] Chenxi Li[c] and Yan Lu*[a]

[a]School of Materials Science & Engineering, Tianjin Key Laboratory for Photoelectric Materials and Devices, Key Laboratory of Display Materials & Photoelectric Devices, Ministry of Education, Tianjin University of Technology, Tianjin, 300384, China.

[b]School of Chemistry, Chemical Engineering and Materials, Jining University, Qufu, 273155, China.

[c]The Centre of Nanoscale Science and Technology and Key Laboratory of Functional Polymer Materials, Renewable Energy Conversion and Storage Center (RECAST), College of Chemistry, Nankai University, Tianjin, 300071, China.

*Corresponding authors.

E-mail: nlqiu@jnxy.edu.cn (N Qiu); luyan@tjut.edu.cn (Y Lu).

Materials and synthesis.

All reagents and solvents were purchased from commercial suppliers and used without further purification. All the reactions and manipulations were carried out under nitrogen atmosphere. The polymer donor PBDB-T was purchased from Solarmer Material (Beijing) Inc. Nonfullerene acceptor TTIC, TTNC and NINCN was prepared according to the reported literature.[1]

Synthesis of TTNC

TTCHO (200 mg, 0.19 mmol) and NINCN (139 mg, 0.57 mmol) were dissolved in dry $CHCl_3$ (30 mL) and 5 mL dry DMF. The mixture was deoxygenated with nitrogen gas for 10 min, and then TMSCl (124 mg, 1.14 mmol) were added. The mixture stirred at 55℃ for 24 h under the protection of nitrogen gas. Then, the mixture was poured into water (100 mL) and extracted with $CHCl_3$. The organic layer was washed with water, and then dried over anhydrous Na_2SO_4. After removing the solvent, the residue was purified using column chromatography on silica gel employing petroleum ether/$CHCl_3$ (1:3) as an eluent, yielding a dark blue solid (176 mg, 62%). ^{1}H NMR (400 MHz, $CDCl_3$), δ 9.17 (s, 2H), 8.94 (s, 2H), 8.36 (s, 2H), 8.09-8.03 (m, 4H), 7.74 (s, 2H), 7.71-7.66 (m, 4H), 7.20-7.13 (m, 16H), 2.59 (t, 8H), 1.62-1.55 (m, 12H), 1.31-1.25 (m, 20H), 0.87 (t, 12H). ^{13}C NMR (100 MHz, $CDCl_3$), δ 187.97, 159.81, 159.44, 155.86, 154.47, 142.59, 140.52, 140.45, 139.66, 138.64, 137.87, 137.34, 135.83, 134.95, 134.38, 132.46, 130.25, 129.77, 129.43, 129.17, 128.69, 127.20, 126.43, 124.00, 122.96, 115.09, 115.01, 66.46, 61.85, 35.22, 31.31, 30.89, 29.33, 28.71, 22.20, 13.72. HR-MS (MALDI): m/z $[M]^+$ calcd for $C_{90}H_{80}N_4O_2S_4$, 1476.5477, found, 1476.5495.

Measurements and Instruments

The ^{1}H and ^{13}C nuclear magnetic resonance (NMR) spectra were taken on a Bruker AV400 Spectrometer. High resolution mass spectrometry (HR-MS) data were recorded on Bruker solariX XR FTMS. The thermogravimetric analysis (TGA) was carried out on a NETZSCH STA 409PC instrument under purified nitrogen gas flow. The heating rate for TGA testing is 10 °C min^{-1}. The UV-*vis* spectra in dilute chloroform solution and films were tested on Agilent Technologies Cary 5000 spectrophotometer. Cyclic voltammetry (CV) experiments were performed with a LK98B II Microcomputer-based Electrochemical Analyzer in dichloromethane solutions. All measurements were carried out at room temperature with a conventional three-electrode configuration employing a glassy carbon electrode as the working electrode, a saturated calomel electrode (SCE) as the reference electrode, and a Pt wire as the counter electrode. Tetrabutylammonium phosphorus hexafluoride (n-Bu_4NPF_6, 0.1 M) in CH_3CN was used as the supporting electrolyte, and the scan rate was 100 mV s^{-1}. The highest occupied molecular orbital (HOMO) and lowest unoccupied molecular orbital (LUMO) energy levels were calculated from the onset oxidation potential and reduction potential by the equation $E_{HOMO} = -(4.80+E_{ox}^{onset})$ and $E_{LUMO} = -(4.80+E_{re}^{onset})$, respectively.

The geometry structures of TTNC were optimized by DFT calculations (B3LYP/6-31G(d,p)), and the frequency analysis was followed to assure that the optimized structures were stable states. All calculations were carried out using Gaussian 09. Atomic force microscope (AFM) investigation was performed using Bruker MultiMode 8 in tapping mode. The transmission electron microscopy (TEM) investigation was performed on Philips Technical G2 F20 at 200 kV. Grazing incidence wide angle X-ray scattering (GIWAXS) was performed at beamline BL14B1 at Shanghai Synchrotron Radiation Facility (SSRF).

The hole and electron mobility were measured using the space charge limited current (SCLC) method, employing a diode configuration of ITO/PEDOT:PSS/active layer/Au for hole and ITO/ZnO/active layer/Al for electron by taking the dark current density in the range of 0-8 V and fitting the results to a space charge limited form, where SCLC is described by:

$$J = \frac{9\varepsilon_0\varepsilon_r\mu_0 V^2}{8L^3}$$

where J is the current density, L is the film thickness of the active layer, μ is the hole or electron mobility, ε_r is the relative dielectric constant of the transport medium, ε_0 is the permittivity of free space (8.85×10^{-12} F m^{-1}), V ($=V_{appl} - V_{bi}$) is the internal voltage in the device, where V_{appl} is the applied voltage to the device and V_{bi} is the built-in voltage due to the relative work function difference of the two electrodes.

The current density-voltage (J-V) characteristics of photovoltaic devices were obtained using a Keithley 2400 source-measure unit. The photocurrent was measured under illumination simulated 100 mW cm^{-2} AM 1.5G irradiation using a xenon-lamp based solar simulator [Oriel 96000 (AM1.5G)] in an argon filled glove box. The external quantum efficiency (EQE) curve was obtained by a QE-R Solar Cell Spectral Response Measurement System.

Solar Cell Fabrication and Characterization

The photovoltaic devices were fabricated with a structure of glass/ITO/PEDOT:PSS/Donor:Acceptor/PDINO/Al. The ITO-coated glasses were cleaned using a detergent scrub, and subsequently subjected to ultrasonic treatment in soap water, deionized water, acetone and isopropyl alcohol for 15 min in each step. After drying by a nitrogen flow, the ITO substrates were treated by ultraviolet-ozone for 15 min. Then, PEDOT:PSS was spin-coated onto the cleaned ITO surface at 4500 rpm for 20 s. The substrates were then placed into a nitrogen-filled glove box after being baked at 150 °C for 20 min. Subsequently, the chloroform solution including donor (10 mg/mL) and TTNC (various concentration based on different D/A weight ratio) was spin-coated at 1700 rpm for 20 s on the ITO/PEDOT:PSS substrate. And then, PDINO, with the concentration of 1.0 mg/mL in CH_3OH was spin-coated at 3000 rpm for 20 s on the active layer. Finally, under the high vacuum, a cathode material Al was deposited onto PDINO layer. The effective area of each cell was 4 mm^2 for the solar cell devices.

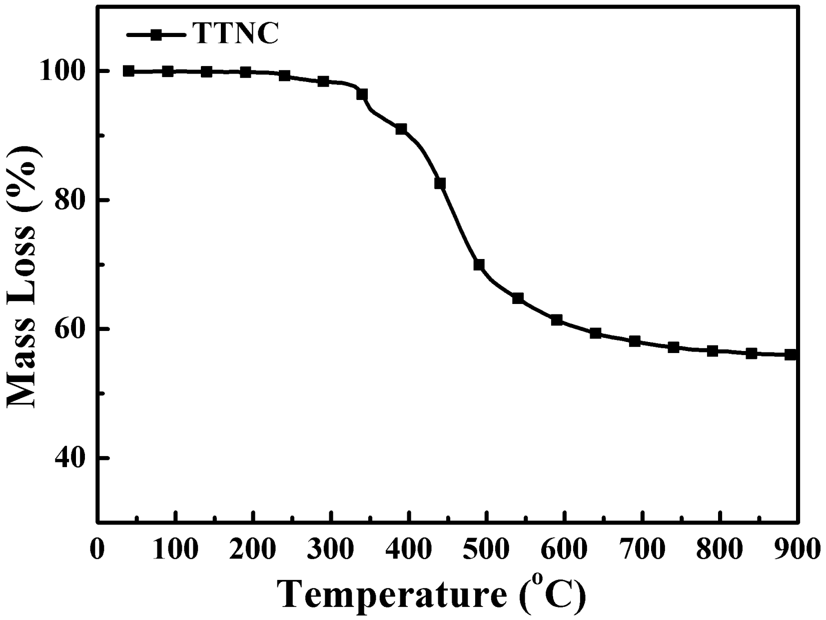

Fig. S1. TGA plot of TTNC.

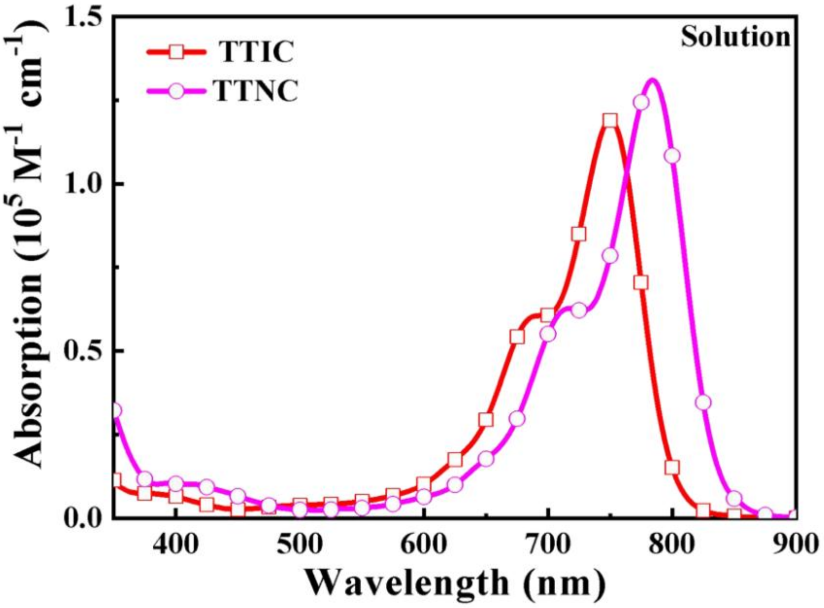

Fig. S2. UV-vis absorption spectra of TTIC and TTNC in chloroform solution.

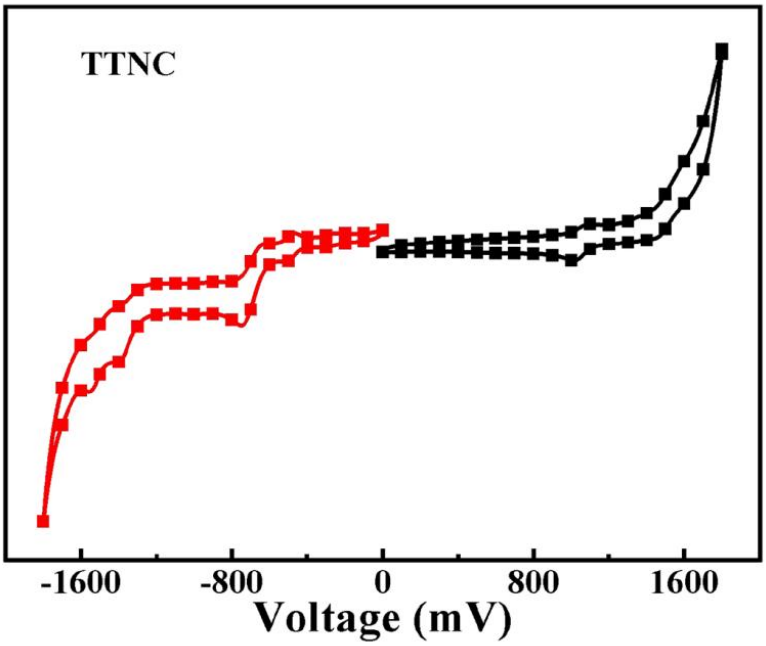

Fig. S3. Cyclic voltammogram of TTNC in acetonitrile with 0.1 mol L^{-1} n-Bu$_4$NPF$_6$.

Table S1. Photovoltaic performance of the solar cells based on PBDB-T:TTNC with different D/A weight ratio.

D:A (w/w)	V_{oc} (V)	J_{sc} (mA cm^{-2})	FF%	PCE (%)
1:0.8	0.75	18.32	67.4	9.26
1:1	0.75	18.92	66.5	9.45
1:1.2	0.75	19.13	63.1	9.05

Table S2. Photovoltaic performance of the solar cells based on PBDB-T:TTNC(1:1, w/w) blend films with different volume ratio of DIO additive in $CHCl_3$.

V%	V_{oc} (V)	J_{sc} (mA cm^{-2})	FF%	PCE (%)
none	0.75	18.92	66.5	9.45
0.1	0.76	20.35	70.4	10.89
0.3	0.76	20.95	71.2	11.34
0.5	0.78	20.67	69.8	11.25

Table S3. Photovoltaic performance of the solar cells based on PBDB-T:TTNC(1:1, w/w) blend films with different additives (0.3 V%).

Additives	V_{oc} (V)	J_{sc} (mA cm^{-2})	FF(%)	PCE (%)
DIO	0.76	20.95	71.2	11.34
Ph-N	0.75	20.88	64.5	10.10
DSH	0.77	19.55	69.7	10.49

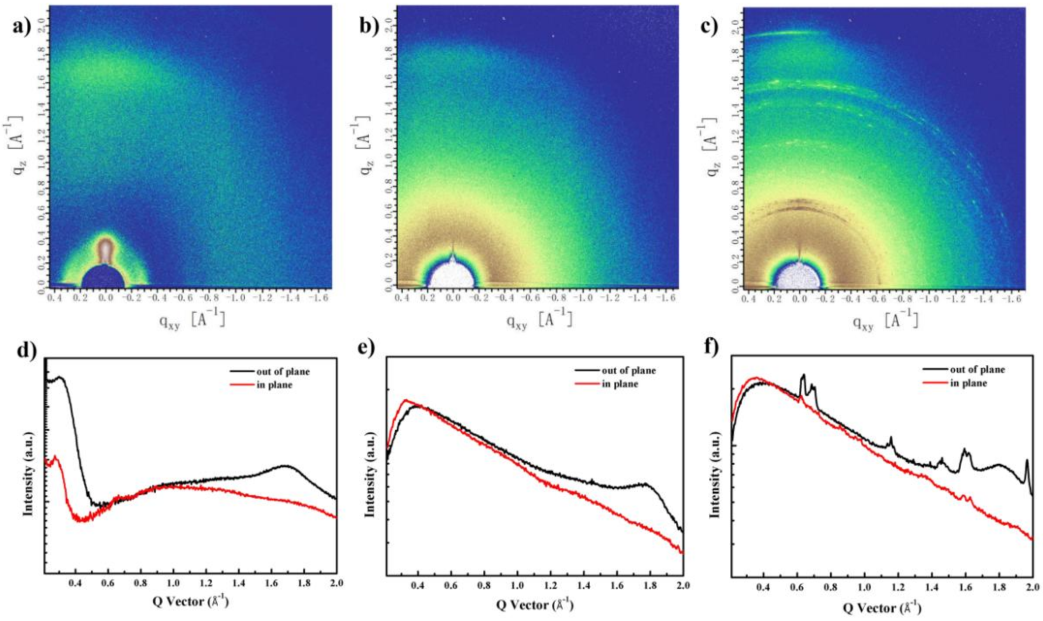

Fig. S4. 2D GIWAXS images of PBDB-T (a), TTIC (b) and TTNC (c) neat films. The corresponding out-of-plane (black line) and in-plane (red line) line-cut profiles (d), (e) and (f).

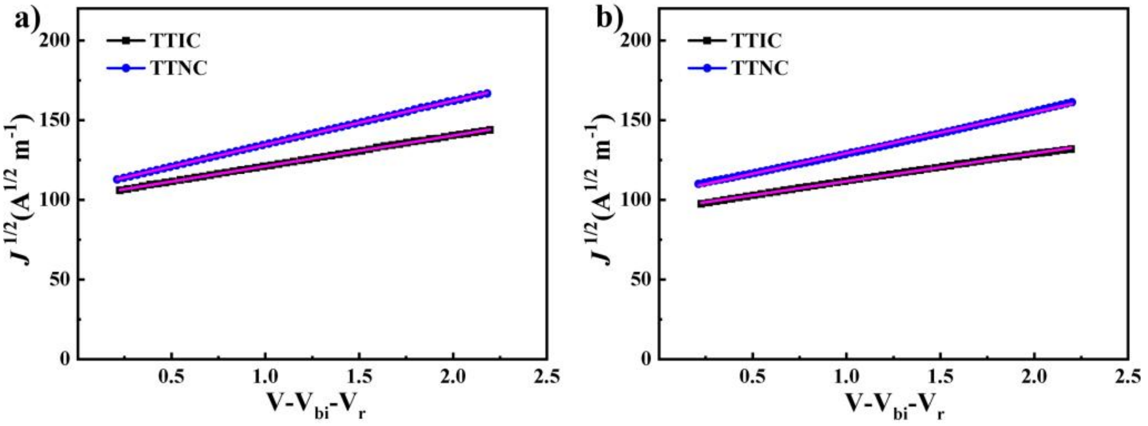

Fig. S5. Hole-only (a) and Electron-only (b) devices based on PBDB-T:TTIC and PBDB-T:TTNC.

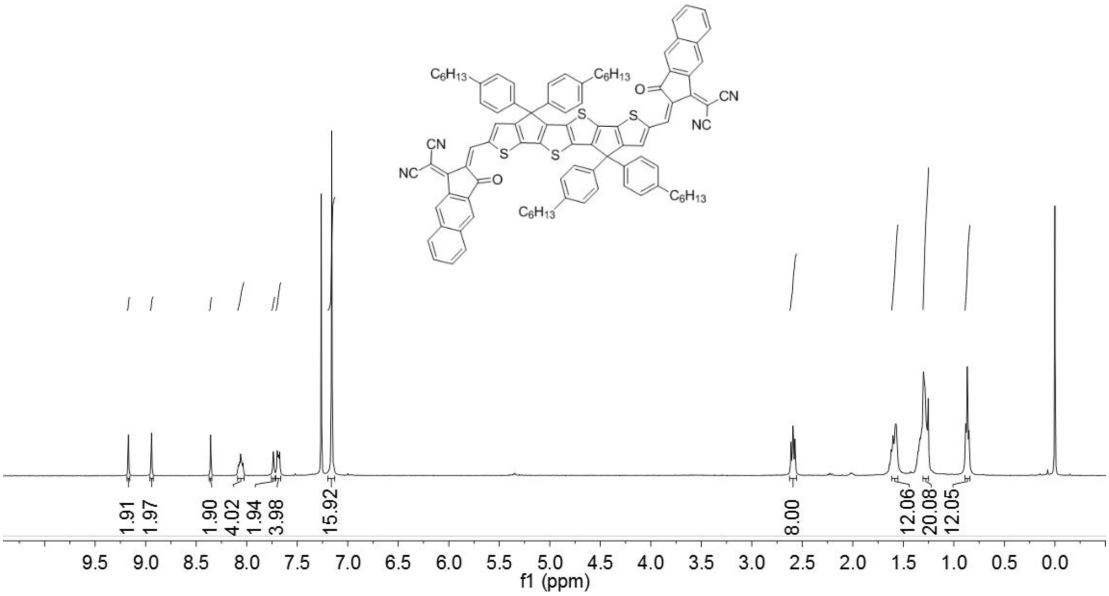

Fig. S6. ^{1}H NMR spectrum of TTNC at 300K in CDCl$_3$.

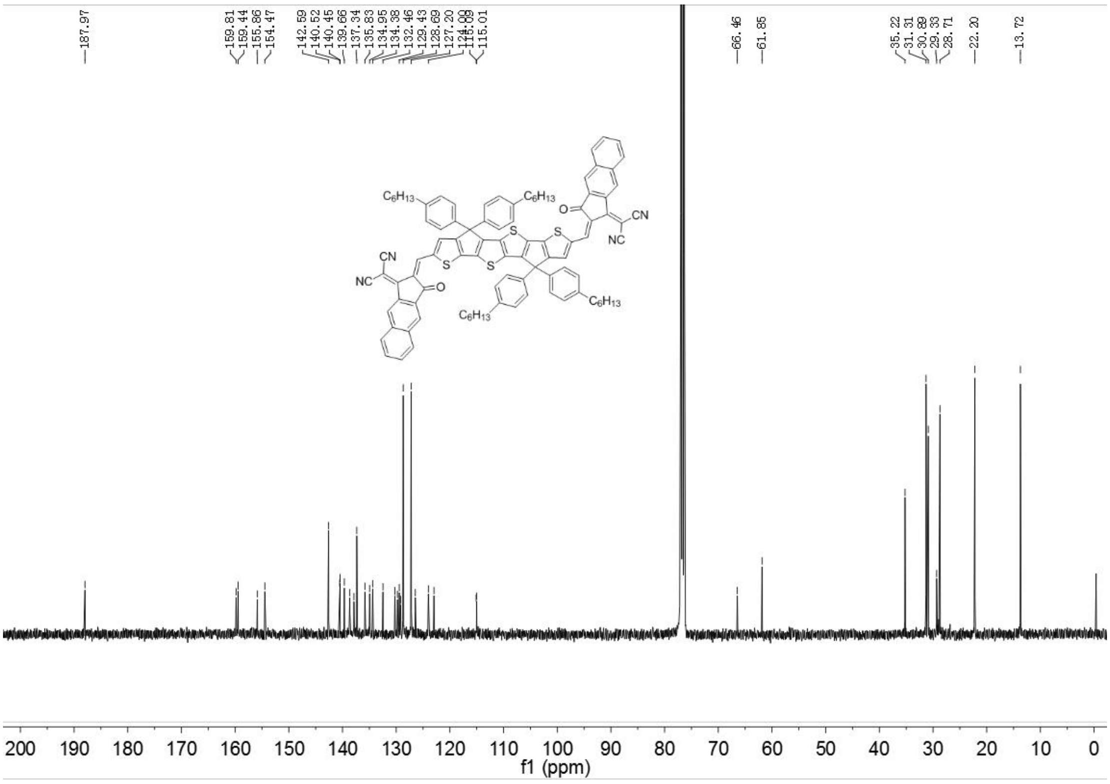

Fig. S7. ^{13}C NMR spectrum of TTNC at 300K in CDCl$_3$.

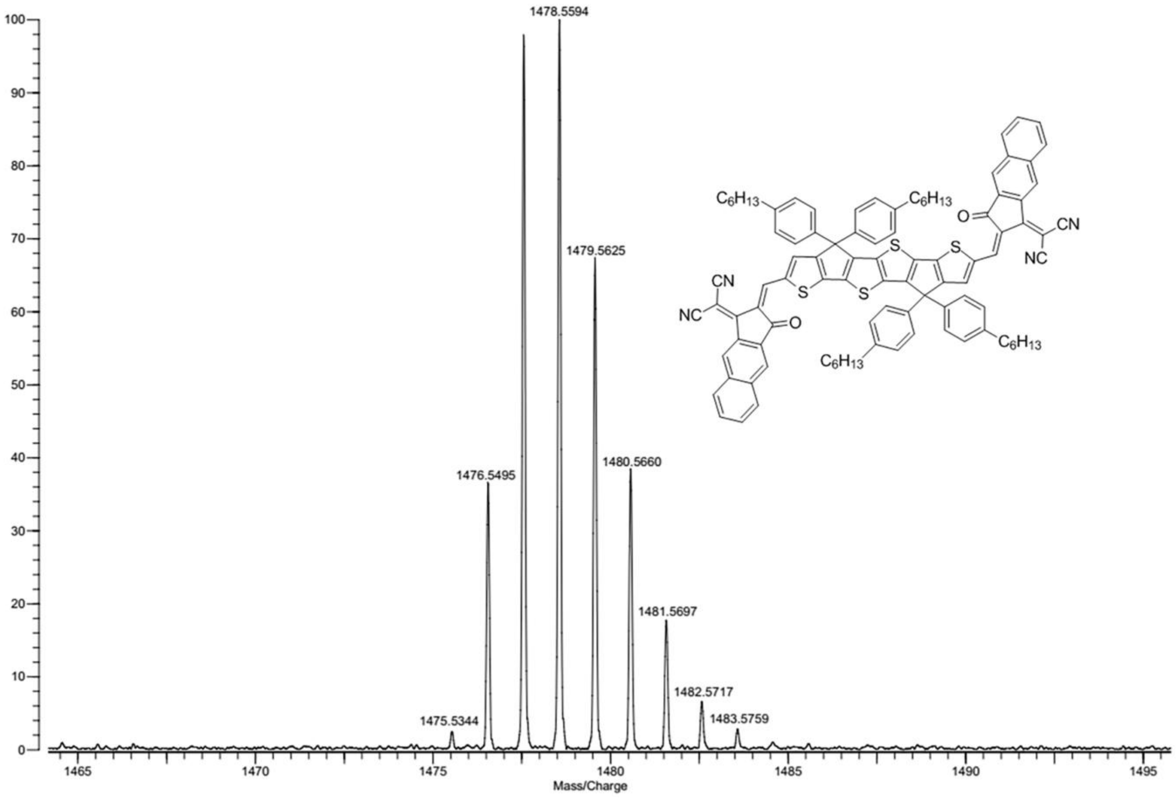

Fig. S8. HR-MS plot of compound TTNC.

References

1. H. Feng, N. Qiu, X. Wang, Y. Wang, B. Kan, X. Wan, M. Zhang, A. Xia, C. Li, F. Liu, H. Zhang and Y. Chen, *Chem. Mater.*, 2017, **29**, 7908-7917.